Journal of Geodesy (2001) 74: 783–795

Journal of Geodesy

Gravitational attraction of local crustal masses in spherical coordinates

D. A. Smith[1], D. S. Robertson[2], D. G. Milbert[1]

[1] National Oceanic and Atmospheric Administration/National Geodetic Survey,
1315 East–West Highway, Silver Spring, Md 20910, USA
e-mail: dru@ngs.noaa.gov, dennis@ngs.noaa.gov; Tel.: +1 301 713 3202; Fax: +1 301 713 4172
[2] National Oceanic and Atmospheric Administration/National Geodetic Survey, CIRES, Campus Box 216,
University of Colorado, Boulder, CO 80309, USA
e-mail: doug@tmgo.colorado.edu; Tel.: +1 303 492 3694; Fax: +1 303 492 5070

Received: 25 October 1999 / Accepted: 15 September 2000

Abstract. The gravitational attractions of terrestrial masses and condensed terrestrial masses were modeled in local regions of gravity stations in different ways. These differences in the models included the type of coordinate frame (Cartesian versus spherical), grid spacing (30 vs 3 arcseconds), and the shape of the terrain (''flat-topped'' vs ''sloped-topped'' prisms). The effect of each of these variables is quantified for its overall impact on Helmert gravity anomalies. The combined effect of removing the masses and restoring the condensed masses is also compared to classical terrain corrections for suitability in computing Helmert anomalies. Some detailed conclusions are drawn from these test computations. The effect of the Earth's curvature has both a near-field effect (due to the differences in volume and shape between rectangular and spherical prisms) and a far-field effect (due to physical location of masses below the horizon). The near-field effect can achieve 0.4 mGal in the Rocky mountains, and affect the geoid by up to 7.5 cm. Additionally, the approximation of the terrain by flat-topped prisms (even at fine spacings such as 3 arcseconds) is inappropriate for terrain near the station, where errors of 20 mGal have been computed using 30-arcsecond data. It is concluded that when 30-arcsecond terrain is allowed to have a more curved (bilinear) prism top, its gravitational attraction is a significantly closer approximation of 3-arcsecond terrain, even for the prism surrounding the station, as compared to the case of 30-arcsecond flat-topped prisms. It is suggested that classical terrain corrections, for many reasons, should not be used to compute Helmert anomalies. Considering only the accuracy, and not the speed, of the computations, the following conclusions are drawn: terrain effects computed inside a local ''cap'' should be done exclusively in spherical coordinates with a 3-arcsecond Digital Elevation Model (DEM) out to 0.2° radius, and then a 30-arcsecond DEM from 0.2 out to 3.5°. In all cases, bilinearly shaped prism tops should be used.

Correspondence to: D. Smith

Key words: Helmert gravity anomalies – Terrain correction – Digital elevation model – Geoid

1 Introduction

The use of the Stokes integral (Heiskanen and Moritz 1967) to solve for the location of the geoid requires a potential field with no masses external to the geoid. Helmert (1884) proposed a few methods for mathematically computing a potential field which fulfills this requirement. Helmert's 2nd method of condensation (Lambert 1930) removes the topographic masses and restores them on a condensed mass layer at the geoid and has the attractive property of having a small indirect effect. However, as pointed out in Martinec (1998, p. 54): ''All existing theories of topographical effects in Helmert's 2nd condensation technique are based on the concept of planar approximation of the geoid.... This approximation describes the actual situation only very roughly''. The emphasis on planar terrain corrections can be seen in the extensive literature on the subject (Blais and Ferland 1983; Smith 1992; Ma and Watts 1994; Leaman 1998). Only recently have spherical effects begun to be studied in great detail (Martinec et al. 1993, 1996; Martinec 1998; Sjöberg and Nahavandchi 1999). In the spirit of Martinec (1998), this paper attempts to further quantify the errors in using planar approximations, as well as to discuss other problems [the coarseness of the Digital Elevation Model (DEM) and the shape of prism tops]. The emphasis of this discussion is on quantifying various approximation-related errors. As such, it is imperative that computational error itself be minimized. Therefore, all computations were done in the space domain in double precision.

In order to use Helmert's 2nd method of condensation in conjunction with the Stokes integral, we must calculate ''Helmert gravity anomalies'' from gravity measurements on the surface of the Earth and a model

of the Earth's topography. Three major gravity reductions (and many smaller ones) are required to do this:

(1) mathematical removal of the topographic masses above the geoid;
(2) mathematical downward continuation of gravity from the Earth's surface to the geoid;
(3) mathematical restoration of the topographic masses as a condensed mass layer on the geoid.

In many past geoid computations, even until recently (i.e. Sideris 1984; Vaníček and Kleusberg 1987; Véronneau 1997; Smith and Milbert 1999), the order of these reductions has been (more or less) as listed but with the first and third reductions combined into the classical terrain correction (TC) and performed in one step (Moritz 1968). The second reduction is classically approximated by a normal gravity gradient or computed using digital terrain models and assuming a linear correlation of elevation with free air gravity anomalies. Recent experiments with spherical Earth models (Milbert and Smith 1998) have shown that the order of these reductions is irrelevant, so long as we adhere to rigorous mathematics. In fact, it is argued that downward continuation should be performed in the smoothest potential field possible. In this case, it should fall between the removal of masses and restoration of condensed masses (smoother potential fields can arguably be obtained by isostatic reductions, but we do not address that issue in this paper). Because the classical TC combines a removal of masses effect at the surface with a restoration of condensed masses effect at the geoid, without allowing a rigorous downward continuation between them, it is seen as a limited tool for high-precision geoid computations. The removal of masses and the restoration of condensed masses are distinct steps, and this paper computes their separate, as well as combined, effects, at a few test locations. This paper does not attempt to address the computation of downward continuation terms, but only to address the terrain issues (that is, reductions 1 and 3 above).

This paper attempts to address the computational issues of removing topographic masses and restoring condensed topographic masses, such as the magnitude of changes on gravity due to (1) the Earth's curvature; (2) the shape of prism tops (flat vs sloped); and (3) the grid spacing of the DEM. In addition, the trade off between acceptable accuracy and computational speed is investigated. This paper confines results to a spherical cap of small (3.5° or less) radius. Terrain effects outside such a cap are long-wavelength, and methods for computing them are being investigated separately.

2 Geometry

This section begins with the geometric differences between three-dimensional (3-D) Cartesian and spherical prisms, specifically the different formulas for computing gravimetric attraction. A brief discussion on the concept of "condensation" follows, and lastly the derivation of formulas for computing gravimetric attraction of condensed masses.

2.1 Formulas for 3-D prisms

At any point in space (P), the gravitational potential (V_P), generated by a generic volume (Π) of mass with a constant density (ρ), can be written in generic coordinates as

$$V_P = G\rho \int_{\Pi} \frac{1}{l}\, \mathrm{d}\Pi \tag{1}$$

where l is the distance from point P to the differential volume element $\mathrm{d}\Pi$ and G is the Newtonian gravitational constant. This formula may be written in Cartesian coordinates as

$$V(x_P, y_P, z_P) = G\rho \int_{\Pi} \frac{1}{\left[(x-x_p)^2 + (y-y_p)^2 + (z-z_p)^2\right]^{(1/2)}}\, \mathrm{d}\Pi \tag{2}$$

where

$\mathrm{d}\Pi = \mathrm{d}x\,\mathrm{d}y\,\mathrm{d}z$
(x, y, z) = local Cartesian coordinates of $\mathrm{d}\Pi$ (z is up)
(x_P, y_P, z_P) = local Cartesian coordinates of P.

The vertical component of gravitational attraction at $P(g_P)$ due to the same mass can be determined through differentiation in the vertical component

$$g(x_P, y_P, z_P) = -\frac{\partial}{\partial z_P} V(x_P, y_P, z_P) \tag{3}$$

written in Cartesian coordinates as

$$g(x_P, y_P, z_P) = -G\rho \int_{\Pi} \frac{(z-z_p)}{\left[(x-x_p)^2 + (y-y_p)^2 + (z-z_p)^2\right]^{(3/2)}}\, \mathrm{d}\Pi \tag{4}$$

If Π is considered a "Cartesian prism" (i.e. a six-faced figure bounded by the plane $x = x_1$ or x_2, the plane $y = y_1$ or y_2, and the surfaces of $z = z_1$ or z_2), then this formula expands to

$$g(x_P, y_P, z_P) = -G\rho \times \int_{x=x_1}^{x_2} \int_{y=y_1}^{y_2} \int_{z=z_1}^{z_2} \frac{(z-z_p)}{\left[(x-x_p)^2 + (y-y_p)^2 + (z-z_p)^2\right]^{(3/2)}}\, \mathrm{d}x\mathrm{d}y\mathrm{d}z \tag{5}$$

where z_1 is often taken to be a constant while z_2 can be a constant (this case will be called "flat-top") or else a

function of x and y (this case will be called "sloped top"). See Figs. 1 and 2 for examples.

In the flat-top case, closed formulas (Nagy 1966) have long been known for solving Eq. (5) (setting x_p, y_p, and z_p to zero for simplicity)

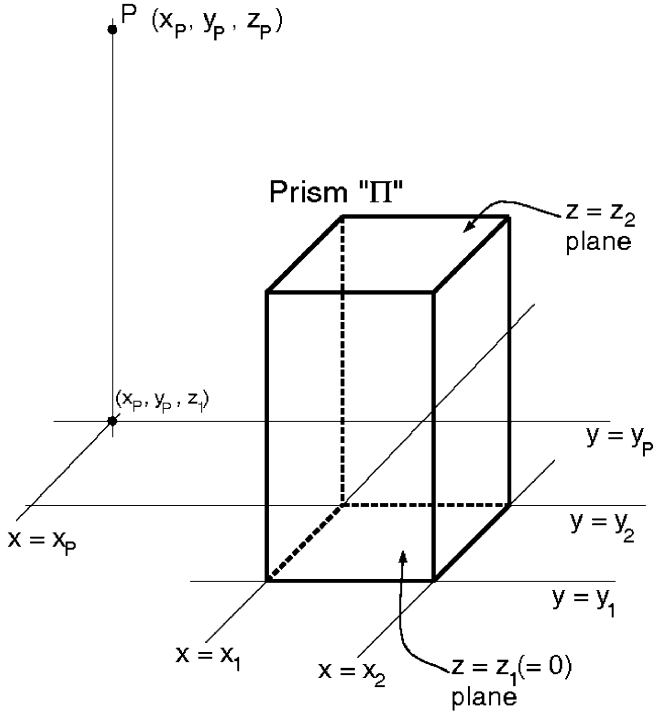

Fig. 1. Example of a Cartesian flat-topped prism

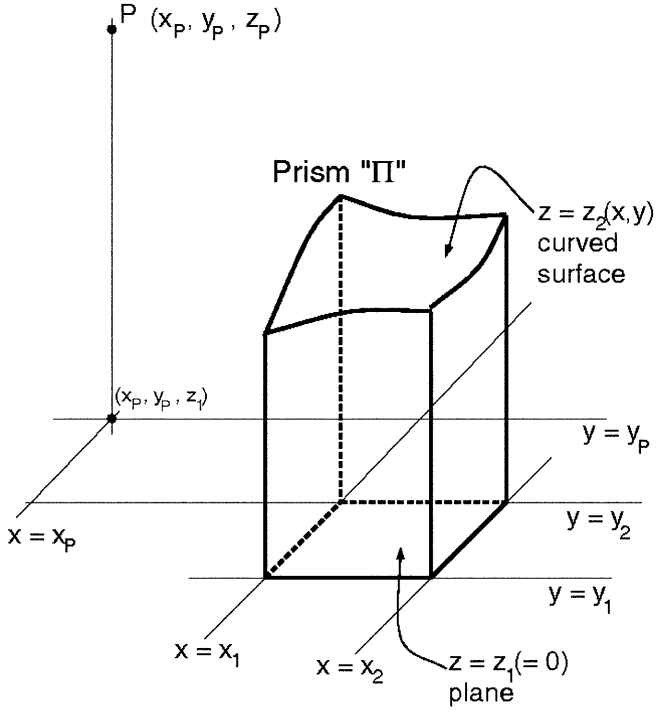

Fig. 2. Example of a Cartesian slope-topped prism

$$g(x_p,y_p,z_p) = -G\rho \sum_{i=1}^{2}\sum_{j=1}^{2}\sum_{k=1}^{2}(-1)^{(i+j+k)} \times \left[-x_i \ln(y_j+s) - y_j \ln(x_i+s) + z_k \arctan\left(\frac{x_i y_j}{z_k s}\right)\right] \quad (6)$$

where

$$s = (x_i^2 + y_j^2 + z_k^2)^{(1/2)} \quad (7)$$

In the case of a sloped top, the simplest surface to fit to the four corner heights of the prism is a bilinear surface, i.e.

$$z_2 = a + bx + cy + dxy \quad (8)$$

In this case, however, no closed solution to the integral has yet been found. [Attempts by the authors to use the symbolic language Mathematica 4.0 (Wolfram 1999) have failed thus far.]

Equation (1) can be written in spherical coordinates, $\phi/\lambda/r$ (in order to model the terrain more accurately than with the use of a "planar" model), as

$$V(\varphi_P,\lambda_P,r_P) = -G\rho \int_{\Pi} \frac{1}{[r^2 + r_P^2 - 2rr_P\cos\psi]^{(1/2)}}\,\mathrm{d}\Pi \quad (9)$$

where

$$\mathrm{d}\Pi = r^2\cos\varphi\,\mathrm{d}\varphi\,\mathrm{d}\lambda\,\mathrm{d}r$$

(φ,λ,r) = geocentric spherical coordinates of $\mathrm{d}\Pi$

$(\varphi_P,\lambda_P,r_P)$ = geocentric spherical coordinates of P

ψ = geocentric angle between P and $\mathrm{d}\Pi$

$$= \arccos[\sin\varphi\sin\varphi_P + \cos\varphi\cos\varphi_P\cos(\lambda-\lambda_P)]$$

Again, through differentiation in the vertical component (r_P)

$$g(\varphi_P,\lambda_P,r_P) = -\frac{\partial}{\partial r_P} V(\varphi_P,\lambda_P,r_P) \quad (10)$$

we may arrive at the gravitational attraction due to this mass, at point P, this time in spherical coordinates

$$g(\varphi_p,\lambda_p,r_p) = -G\rho \int_{\Pi} \frac{(r\cos\psi - r_p)}{(r^2 + r_p^2 - 2rr_p\cos\psi)^{3/2}}\,\mathrm{d}\Pi \quad (11)$$

If Π is considered a "spherical prism" (i.e. a six-faced figure bounded by meridians of $\lambda = \lambda_1$ or λ_2, parallels of $\phi = \phi_1$ or ϕ_2, and curved surfaces of $r = r_1$ or r_2), then Eq. (11) expands to

$$g(\varphi_p,\lambda_p,r_p) = -G\rho \int_{\varphi=\varphi_1}^{\varphi_2}\int_{\lambda=\lambda_1}^{\lambda_2}\int_{r=r_1}^{r_2} \frac{(r\cos\psi - r_p)r^2\cos\varphi}{(r^2 + r_p^2 - 2rr_p\cos\psi)^{(3/2)}}\,\mathrm{d}r\,\mathrm{d}\lambda\,\mathrm{d}\varphi \quad (12)$$

where r_1 may be taken to be a constant radius R. Again there are the two cases of "flat-top" (r_2 is a constant) and "sloped top" (r_2 as a function of ϕ and λ). See Figs. 3 and 4 for examples.

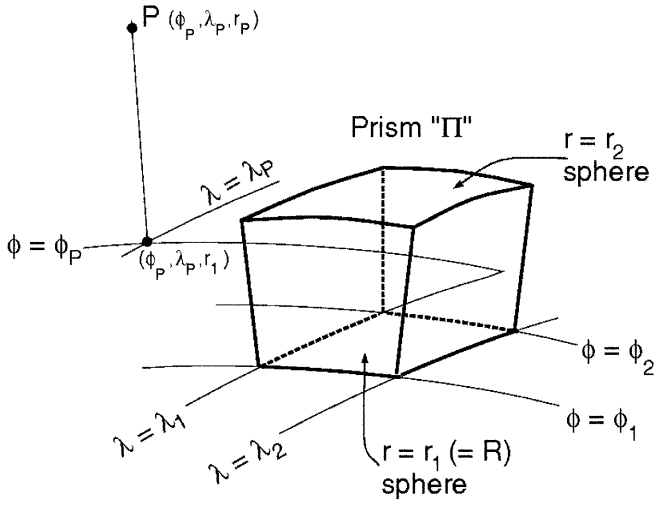

Fig. 3. Example of a spherical flat-topped prism

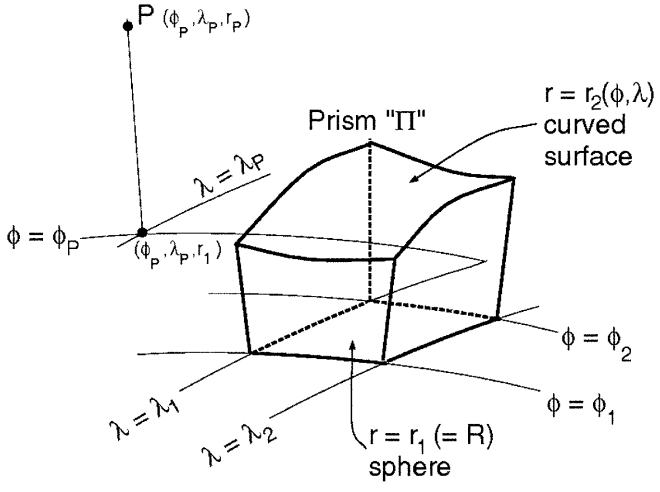

Fig. 4. Example of a spherical slope-topped prism

Although no closed form has yet been found for the solution to the triple integral in Eq. (12), the integral with respect to r can be removed to speed up numerical integration, using the following formula (see also Martinec 1998, p 45):

$$g(\varphi_p,\lambda_p,r_p) = -G\rho \int_{\varphi=\varphi_1}^{\varphi_2}\int_{\lambda=\lambda_1}^{\lambda_2} \cos\varphi \left[\frac{\left(rr_p - 6\cos^2\psi rr_p + \cos\psi(r^2+3r_p^2)\right)}{l} - (1-3\cos^2\psi) r_p \ln(r - r_p\cos\psi + l) \right]_{r=r_1}^{r=r_2} \mathrm{d}\lambda\,\mathrm{d}\varphi \tag{13}$$

where

$$l = \sqrt{r^2 + r_p^2 - 2rr_p\cos(\psi)} \tag{14}$$

The formulas presented thus far represent gravitational potential and attraction of 3-D prisms. The point at which the 3-D attractions are computed was referred to as point P. In Helmert's 2nd method of condensation, we must also be concerned with the gravitational attractions of those same prisms as condensed into two dimensions. The concept of "condensing" 3-D masses into 2-D condensed mass layers is discussed in the next section.

2.2 Mass condensation

Helmert's 2nd method of condensation is a scheme whereby the 3-D masses above the geoid are "condensed" along the vertical direction (z in Cartesian, r in spherical) to form a 2-D mass layer on the geoid. The concept is fairly simple, but there are some differences between condensation in Cartesian and spherical coordinates. In both cases, a differentially small column of mass is first defined [bounded by $(x, x+\mathrm{d}x)$, $(y, y+\mathrm{d}y)$, (z_1, z_2) in Cartesian coordinates or $(\phi, +\mathrm{d}\phi)$, $(\lambda, \lambda+\cos\phi\,\mathrm{d}\lambda)$, (r_1, r_2) in spherical coordinates], whose projection along the vertical direction onto the geoid is the differential area $\mathrm{d}A$. In the case of Cartesian coordinates, the "geoid" is the plane $z = z_1$, and $\mathrm{d}A$ is

$$\mathrm{d}A = \mathrm{d}x\,\mathrm{d}y \tag{15}$$

In spherical coordinates, the "geoid" is the sphere $r = r_1$, and the differential area $\mathrm{d}A$ is

$$\mathrm{d}A = r_1^2\cos\varphi\,\mathrm{d}\varphi\,\mathrm{d}\lambda \tag{16}$$

The amount of volume in the Cartesian differential column is

$$\begin{aligned}\mathrm{dvol} &= \int_{z=z_1}^{z_2} \mathrm{d}\Pi = \int_{z=z_1}^{z_2} \mathrm{d}x\,\mathrm{d}y\,\mathrm{d}z \\ &= (z_2 - z_1)\mathrm{d}x\,\mathrm{d}y = (z_2 - z_1)\mathrm{d}A\end{aligned} \tag{17}$$

and in the spherical differential column

$$\begin{aligned}\mathrm{dvol} &= \int_{r=r_1}^{r_2} \mathrm{d}\Pi = \int_{r=r_1}^{r_2} r^2\cos\varphi\,\mathrm{d}\varphi\,\mathrm{d}\lambda\,\mathrm{d}r \\ &= \frac{1}{3}(r_2^3 - r_1^3)\cos\varphi\,\mathrm{d}\varphi\,\mathrm{d}\lambda = \frac{(r_2^3 - r_1^3)}{3r_1^2}\mathrm{d}A\end{aligned} \tag{18}$$

Since mass must be conserved in condensation, the amount of mass that is in the 3-D differential columns must be equal to the mass that is contained in the differential area $\mathrm{d}A$ after condensation. As such, we can use this mass conservation to compute the surficial density, κ (kg/m^2), of the condensed masses in terms of the old density, ρ, and the height, H, of the differential column. In Cartesian coordinates (with $H = z_2 - z_1$)

$$\begin{aligned}\mathrm{d}M(3-D) &= \mathrm{d}M(2-D) \\ &\Rightarrow \rho\,\mathrm{dvol} = \kappa\,\mathrm{d}A \\ &\Rightarrow \rho(z_2 - z_1)\mathrm{d}A = \kappa\,\mathrm{d}A \\ &\Rightarrow \rho(H)\mathrm{d}A = \kappa\,\mathrm{d}A\end{aligned} \tag{19}$$

and thus in Cartesian coordinates

$$\kappa = \rho H \tag{20}$$

and in spherical coordinates (with $H = r_2 - r_1$)

$$\begin{aligned} \mathrm{d}M(3-D) &= \mathrm{d}M(2-D) \\ &\Rightarrow \rho\,\mathrm{dvol} = \kappa\,\mathrm{d}A \\ &\Rightarrow \rho(r_2^3 - r_1^3)/(3r_1^2)\mathrm{d}A = \kappa\,\mathrm{d}A \\ &\Rightarrow \rho\left(H + \frac{H^2}{r_1} + \frac{H^3}{3r_1^2}\right)\mathrm{d}A = \kappa\,\mathrm{d}A \end{aligned} \tag{21}$$

Therefore, in spherical coordinates

$$\kappa = \rho\left(H + \frac{H^2}{r_1} + \frac{H^3}{3r_1^2}\right) \tag{22}$$

Note the 2nd and 3rd terms in Eq. (22), which are missing from Eq. (20). By neglecting the 2nd and 3rd terms of Eq. (22), a maximum error of 0.15% is introduced, depending on the magnitude of H. This error, however, is systematic and, like all systematic errors, should not be ignored. In the US, preliminary tests indicate that the systematic nature of this error can sum up to geoid errors of a few cm.

2.3 Formulas for 2-D condensed prisms

In this paper, the point at which the attraction of the condensed masses will be computed is referred to as point P_0 (which may or may not be the same as point P, depending on the sequence of gravity reductions). However, P_0 will always lie along the same vertical as P [so that the horizontal coordinates (x, y) or (ϕ, λ) are identical for P and P_0]. The gravitational potential of such a condensed prism, at a point P_0, can be written generically as

$$V_{P_0} = G\int_A \frac{\kappa}{l}\,\mathrm{d}A \tag{23}$$

where l is the distance from point P_0 to the differential area element $\mathrm{d}A$, G is the Newtonian gravitational constant, and κ is the surficial density of the condensed layer (kg/m^2). This formula may be written in Cartesian coordinates as

$$V(x_{P_0}, y_{P_0}, z_{P_0}) = G\int_A \frac{\kappa}{\left[(x-x_{P_0})^2 + (y-y_{P_0})^2 + (z_1 - z_{P_0})^2\right]^{(1/2)}}\,\mathrm{d}A \tag{24}$$

where

$\mathrm{d}A = \mathrm{d}x\,\mathrm{d}y$

(x, y, z_1) = local Cartesian coordinates of $\mathrm{d}A$

$(x_{P_0}, y_{P_0}, z_{P_0})$ = local Cartesian coordinates of P_0

κ is not removed from the integral, since it depends on z_2, which may depend on x and y in the "sloped-top" case. Using Eq. (20), Eq. (24) can be expanded slightly to

$$V(x_{P_0}, y_{P_0}, z_{P_0}) = G\rho\int_A \frac{(z_2 - z_1)}{\left[(x-x_{P_0})^2 + (y-y_{P_0})^2 + (z_1 - z_{P_0})^2\right]^{(1/2)}}\,\mathrm{d}A \tag{25}$$

The gravitational attraction of such a condensed prism at a point P_0 can be computed, as before, through differentiation of potential in the vertical component

$$g(x_{P_0}, y_{P_0}, z_{P_0}) = -\frac{\partial}{\partial z_{P_0}} V(x_{P_0}, y_{P_0}, z_{P_0}) \tag{26}$$

written in Cartesian coordinates as

$$g(x_{p_0}, y_{p_0}, z_{p_0}) = -G\rho\int_{x=x_1}^{x_2}\int_{y=y_1}^{y_2} \frac{(z_2 - z_1)(z_1 - z_{p_0})}{\left[(x-x_{p_0})^2 + (y-y_{p_0})^2 + (z_1 - z_{p_0})^2\right]^{(3/2)}}\,\mathrm{d}y\,\mathrm{d}x \tag{27}$$

Equations (26) and (27) are smooth and continuous as long as $z_{P_0} \neq z_1$ (station is not "on" the condensed layer). In the flat-top prism case, a closed-form solution to this equation (setting $x_{p_0}, y_{p_0}, z_{p_0}$ all to zero) is as shown below

$$g(x_{p_0}, y_{p_0}, z_{p_0}) = -G\rho(z_2 - z_1)\sum_{i=1}^{2}\sum_{j=1}^{2}(-1)^{(i+j)}\arctan\left[\frac{x_i y_j}{z_1 s}\right] \tag{28}$$

where

$$s = (x_i^2 + y_j^2 + z_1^2)^{(1/2)} \tag{29}$$

A quick examination of Eq. (27) shows that if the station (z_{p_0}) is at the same height as the condensed layer (z_1) then there will be no vertical gravitational attraction due to the condensed layer. [That is, Eqs. (27) and (28) are discontinuous at the condensed layer.] This is in disagreement with the traditional planar (Cartesian) implementation of Helmert's 2nd method of condensation, if the condensed prism is directly below the station ($x_1 \le x_P \le x_2$ and $y_1 \le y_P \le y_2$). If it is to the side, then in Cartesian coordinates it is expected that there should not be any vertical gravitational attraction due to the condensed layer. In the case where the condensed prism is directly below the station, a limit is used to compute the attraction of the condensed masses as P_0 is moved progressively closer to the condensed layer

$$\lim_{z_{p_0} \mapsto z_1} g(x_{p_0}, y_{p_0}, z_{p_0}) = \begin{cases} -2\pi G\rho H & \text{prism below station} \\ 0 & \text{prism to side of station} \end{cases} \tag{30}$$

The limit used here is one-sided, allowing the point P_0 to approach the "geoid" (surface upon which the condensed masses reside) from above ($+z$ or $+r$ direction). The limit represents the gravitational attraction at a point P_0 that is an infinitesimally small distance above the geoid. This is desirable, as the value of gravitational attraction is discontinuous (though not necessarily undefined) at the location of condensed masses. The fact that this "limiting value" is required, and not the value directly on the geoid itself, in order to ensure compatibility between various orderings of gravity reductions, was shown in Milbert and Smith (1998).

Similar "condensed attraction" equations need to be derived in spherical coordinates. Beginning with the spherical version of Eq. (23)

$$V(\varphi_{P_0}, \lambda_{P_0}, r_{P_0}) = G \int_A \frac{\kappa}{[(r^2 + r_{P_0}^2 - 2r_1 r_{P_0} \cos\,\psi)]^{(1/2)}} \mathrm{d}A$$

$\mathrm{d}A = r_1^2 \cos\,\varphi\,\mathrm{d}\varphi\,\mathrm{d}\lambda$

(φ, λ, r_1) = geocentric spherical coordinates of $\mathrm{d}A$

$(\varphi_{P_0}, \lambda_{P_0}, r_{P_0})$ = geocentric sphericalcoordinates of P_0

ψ = geocentric angle between P_0 and $\mathrm{d}A$

$$= \arccos[\sin\,\varphi\,\sin\,\varphi_{P_0} + \cos\,\varphi\,\cos\,\varphi_{P_0}\,\cos(\lambda - \lambda_{P_0})] \tag{31}$$

Using Eq. (22), Eq. (31) may be expanded to

$$V(\varphi_{P_0}, \lambda_{P_0}, r_{P_0}) = G\rho \int_A \frac{(r_2 - r_1) + \left(\frac{(r_2-r_1)^2}{r_1}\right) + \left(\frac{(r_2-r_1)^3}{3r_1^2}\right)}{[(r_1^2 + r_{P_0}^2 - 2r_1 r_{P_0} \cos\,\psi)]^{(1/2)}}\,\mathrm{d}A \tag{32}$$

The gravitational attraction of such a condensed prism, at a point P_0, can be computed, as before, through differentiation of potential in the vertical component

$$g(\varphi_{P_0}, \lambda_{P_0}, r_{P_0}) = -\frac{\partial}{\partial r_{P_0}} V(\varphi_{P_0}, \lambda_{P_0}, r_{P_0}) \tag{33}$$

which fully expands to

$$g(\varphi_{p_0}, \lambda_{p_0}, r_{p_0}) = -G\rho \int_{\varphi=\varphi_1}^{\varphi_2} \int_{\lambda=\lambda_1}^{\lambda_2} \frac{\left[(r_2 - r_1) + \left(\frac{(r_2-r_1)^2}{r_1}\right) + \left(\frac{(r_2-r_1)^3}{3r_1^2}\right)\right](r_1 \cos\,\psi - r_{p_0}) r_1^2 \cos\,\varphi}{(r_1^2 + r_{p_0}^2 - 2r_1 r_{p_0} \cos\,\psi)^{3/2}}\,\mathrm{d}\lambda\,\mathrm{d}\varphi \tag{34}$$

Unlike the case of Cartesian coordinates, the condensed prisms "to the side" of the station do not have a zero contribution as P_0 approaches the condensation surface. This is because the condensation surface, being spherical, allows condensed prisms to lie below the local horizon of any station as that station approaches $r = r_1$. Equation (34) has no known closed-form solution, but the limit as r_{p_0} approaches r_1 may still be applied to it, to achieve the following integral

$$\lim_{r_{p_0} \mapsto r_1} g(\varphi_{p_0}, \lambda_{p_0}, r_{p_0}) = \begin{cases} -2\pi G\rho H - Q & \text{prism below station} \\ 0 - Q & \text{prism to side of station} \end{cases} \tag{35}$$

where

$$Q = -G\rho \times \int_{\varphi=\varphi_1}^{\varphi_2} \int_{\lambda=\lambda_1}^{\lambda_2} \frac{\left[(r_2 - r_1) + \left(\frac{(r_2-r_1)^2}{r_1}\right) + \left(\frac{(r_2-r_1)^3}{3r_1^2}\right)\right]\cos\,\varphi}{2\sqrt{2 - 2\cos\,\psi}}\,\mathrm{d}\lambda\,\mathrm{d}\varphi \tag{36}$$

It should be noted that Eq. (35) is in agreement with the more general derivation given in Heiskanen and Moritz (1967, Eqs. 1–17a).

Since comparisons will be drawn between the formal remove/restoration equations above and classical terrain corrections, the classical TC approximation formula is presented in Eq. (37) below. Recall (Moritz 1968, p 41; see also the Appendix in the present paper) that this equation is used to approximate the overall effect of removing the masses (for a point P at the surface of the Earth) and restoring the condensed masses (for a point P_0 at the geoid).

$$\mathrm{TC} = \frac{1}{2} G\rho \int_{x=-\infty}^{x=+\infty} \int_{y=-\infty}^{y=+\infty} \frac{(H(x,y) - H_p)^2}{l_0^3}\,\mathrm{d}x\,\mathrm{d}y \tag{37}$$

where l_0 is the horizontal distance approximation between (x, y) and (x_P, y_P). As per the comments above, the height of $P_0(z_{P_0})$ is not truly "on" the geoid ($z = z_1$), but is an infinitesimally small distance above it. Note also that this "classical" formula is convenient for computing TCs from Fourier transforms, but it is an approximation to the "true" TC value, in planar coordinates (see Appendix).

To summarize, equations for computing gravitational attraction of 3-D and 2-D (condensed) masses in Cartesian or spherical coordinates have been presented, and closed forms presented where they exist. For the special case where we are interested in the attraction of condensed masses at a point that has been moved from the surface down to the condensation level, limits have been used to show how to compute those attractions. When closed forms for these integrals were not available, the computations in this paper used a Romberg quadrature numerical integration algorithm as specified in Press et al. (1992, pp 155–158).

This paper is focused more on errors due to various terrain approximations, rather than emphasizing com-

putational speed. Ultimately, however, it is desirable to find a reasonable tradeoff between computational accuracy and computational speed that can be used in the processing of terrain-related gravity effects at the millions of gravity stations around the US.

3 Methodology

As mentioned earlier, in order to arrive at Helmert anomalies on the geoid, gravity values on the surface of the Earth must have three primary corrections applied (see Sect. 1). The computations in this paper assume the order as listed in Sect. 1, but this paper does not attempt to address the computation of the 2nd reduction (downward continuation) itself. The order of events is mentioned merely to establish (for this paper) that the "remove step" is performed for a point at one location and the "restore step" is performed for a point that has been moved (downward continued) to another location. No working knowledge of *how* that downward continuation was performed is required to compute these terrain effects. As such, for the remainder of this paper it is assumed that gravitational attractions are computed for 3-D masses at point P (the surface) but for condensed masses at point P_0 (the geoid).

Four methods of computing the remove/restore were used, as follows.

(1) Traditional planar terrain corrections at point P (a single computation which is used to approximate the combined effects of both the remove step, at P, and the restore step, at P_0). [Eq. (37)].
(2) Rigorous remove (P) and restore (P_0) in planar coordinates [Eqs. (6) and (28)].
(3) Same as method 2 but in spherical coordinates [Eqs. (14) and (35)].
(4) Same as method 3 but allowing the tops of the prisms to slope bilinearly [Eqs. (14) and (35), with r_2 varying bilinearly].

In this way, the effect of each geometric change may be monitored directly.

Additionally, the important question of DEM grid spacing was investigated. A 3-arcsecond DEM (based on National Imagery and Mapping Agency Digital Terrain Elevation Data level 1 data) was used both at the 3-arcsecond level, and averaged to the 30-arcsecond level, to investigate the impact of coarseness. Lastly, to provide results that were for general terrain, four areas of varying roughness (as measured through horizontal gradients of terrain) were investigated during this study: Pikes Peak, Colorado (extremely high and extremely rugged), central Colorado (high and moderately rugged), the Appalachians (low and slightly rugged) and the Pacific Northwest (high and extremely rugged).

4 Effect of geometric differences

Computations of gravitational attraction were tabulated in roughly circular rings ("roughly" because the DEM grid is latitude/longitude based and not distance/azimuth based) surrounding a station. The stations used in the four computational areas are outlined in Table 1.

It should be noted that these stations do not fall on even latitude and longitude lines, and their heights do not necessarily lie on any particular surface defined by the DEM data. This is very much the way any other random gravity stations would appear. This raises the issue of what height to use for the gravity station. In most gravity measurements in the National Geodetic Survey (NGS) database, an orthometric height is given, usually scaled from a local topographic map. These heights are usually considered accurate to $+/-3$ m in general (sometimes much worse in the mountains). However, there are many instances where these scaled heights disagree radically (often by hundreds of meters) from various DEMs in the region. In addition, interpolating a height from a 30-arcsecond DEM (which is about 1 km horizontal spacing) can yield standard errors in heights at the $+/-20$ m level, but only $+/-5$ m from a 3-arcsecond DEM (Smith and Roman in press). Because it is important in geoid computations for heights to be consistent (Smith and Milbert 1999; Smith and Roman in press), and because the DEMs generally have fewer blunders than the scaled heights in the gravity database, the height of the station was always determined by bilinearly interpolating from the four grid nodes of the 3-arcsecond DEM surrounding the station. This removes blunders, and gives one consistent station height to which all terrain reductions may accurately refer.

The gravitational attraction, on a ring-by-ring basis, was computed for these stations using the four methods outlined in the previous section. Cumulative graphs of the removal (at P) and restoration (at P_0) for the four methods for central Colorado are shown in Figs. 5 and 6. In all cases, these computations were done with 30-arcsecond DEM data. The conclusions drawn from the Central Colorado test are very similar to those drawn for the other areas. Thus, for conciseness, the focus of this discussion will be on the results from Central Colorado.

Certain conclusions can be drawn from a study of these two figures. First, note that the combined (remove/restore) gravitational attraction computed using method 1 (classic TC) increases monotonically with distance from the station, while that of methods 2, 3, and 4 monotonically decreases. This is to be expected because method 2, by its very nature, includes the restoration of the infinite Bouguer Plate [see Eq. (30)], whereas method 1 would need to be evaluated to infinity to see the complete effect. Because methods 1 and 2 both represent

Table 1. Coordinates of four gravity stations of interest

Name	Latitude (°)	Longitude (°)	Height (m)
Pike's Peak	38.840708	254.958653	4154.13
Central Colorado	38.500139	254.500139	2397.64
Appalachia	37.500417	279.500417	785.75
Pacific Northwest	46.500417	239.500417	491.00

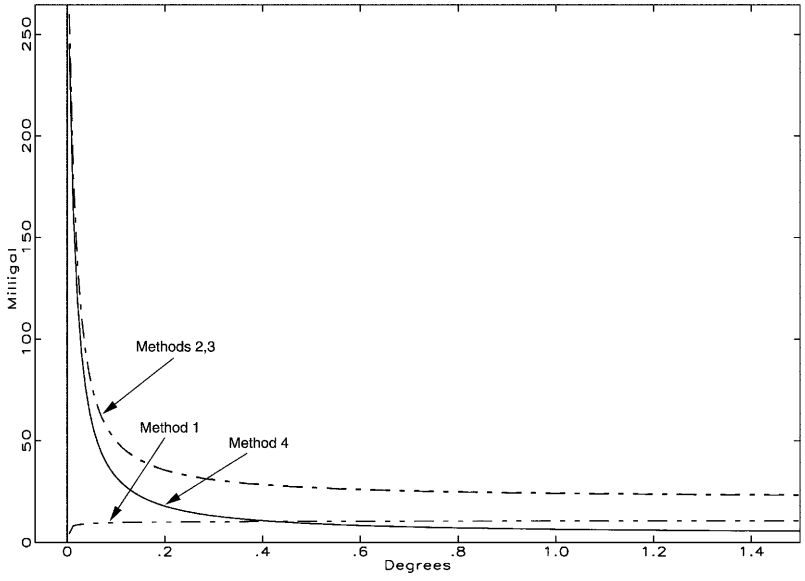

Fig. 5. Combined effect of the removal of gravitational attraction of 3-D masses (computed at the Earth's surface) and the restoration of gravitational attraction of condensed masses (computed at the geoid) for the central Colorado station, 0. to 1.5° from the station, using 30-arcsecond terrain data. Method 1 is shown with *dash-dot-dot*; method 2 with *dash-dot*, method 3 with *dots*, and method 4 with a *solid line*. Note that the scale prevents separation of the lines for methods 2 and 3

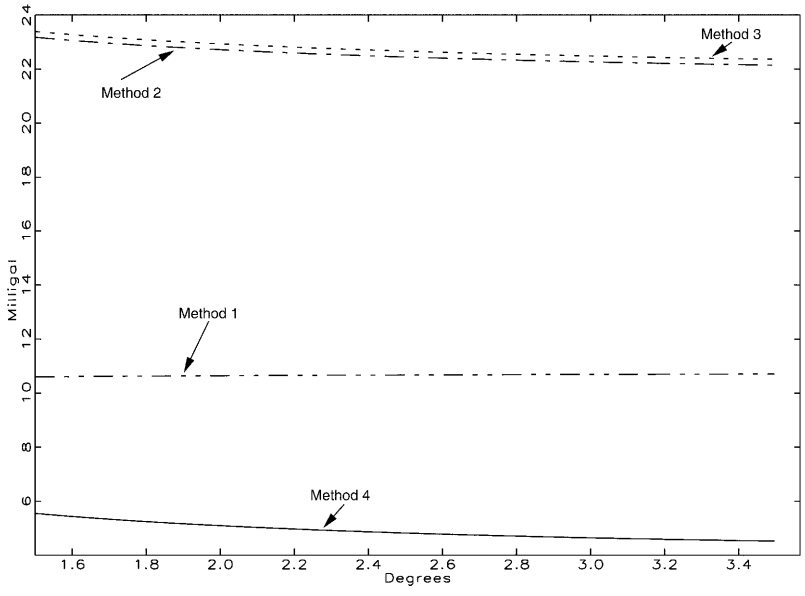

Fig. 6. As Fig. 5, but for 1.5 to 3.5° from the station

the terrain in Cartesian coordinates, it is obvious that if they are both taken to infinity, then their representations of the removal and restoration of the terrain would become identical and they should approach the same limit, but from opposite directions.

Second, there is a nearly 20-mGal offset of method 4 from method 3. This is due entirely to the difference between the flat-top assumption in method 3 and the (bilinear) slope-top assumption in method 4. Most of this difference results from the central prism and its immediate neighbors.

Finally, a small systematic offset exists between methods 2 and 3. This offset is due to two separate effects, both tied to the curvature of the Earth. The first, and dominant, effect will be called the "near-field spherical effect". This effect is due to the different shapes of spherical prisms from rectangular prisms. Differing shapes yield different mass distributions, and subsequently different gravitational attractions of both the 3-D and condensed masses. In fact, the largest contribution to this effect is the difference in gravitational attraction of condensed masses for the one prism directly below any point P. This effect has almost no dependence on the grid spacing (3 vs 30 arcseconds), nor on latitude, but is almost entirely dependent on the height of station P. A few example computations showing the height dependence of this effect, broken down into removal of 3-D masses, restoration of condensed masses, and the combined effect of these two reductions, are shown in Table 2.

In Table 2, the cause of the differences between Cartesian and spherical is mostly due to using a poor κ value in Cartesian coordinates [Eq. (20) vs Eq. (22)]. By picking a poor κ value, the "wrong" amount of condensed mass is put in a very close proximity to point P_0, causing a discrepancy between Cartesian and spherical

Table 2. Numerical examples of near-field spherical effect for 30-arcsecond data (mGal)

H (m)	Cartesian			Spherical			Difference combined
	Remove	Restore	Combined	Remove	Restore	Combined	
100	−9.910	+11.194	1.284	−9.908	+11.194	1.286	0.002
1000	−38.772	+111.940	73.168	−38.774	+111.961	73.187	0.019
5000	−47.175	+559.701	512.526	−47.203	+560.160	512.957	0.431

cases. An empirical function was fitted to the difference between Cartesian and spherical cases of the combined effect of removing 3-D masses at the Earth's surface and restoring condensed masses at the geoid (for heights ranging from 0 to 5000 m). This empirical function is shown in Fig. 7.

Figure 7 represents an error curve, depending on height, that is systematically produced if Cartesian coordinates are used to compute the removal of the 3-D masses at P (surface), and the restoration of condensed masses at P_0 (geoid). This error is designated $\delta\Delta g^{\mathrm{NFSE}}$ (NFSE = near-field spherical effect) and empirically follows the form

$$\delta\Delta g^{\mathrm{NFSE}} = a + bH + cH^2 \tag{38}$$

where $\delta\Delta g^{\mathrm{NFSE}}$ represents the error in using Cartesian coordinates, rather than spherical, to compute the combined effects of removing masses at P (Earth's surface) and restoring condensed masses at P_0 (geoid), in mGal. H represents the height of station P in meters, and

$$\begin{aligned} a &= 0 \pm 0\,\mathrm{mGal} \\ b &= -3.056 \times 10^{-7} \pm 2.178 \times 10^{-7}\,\mathrm{mGal/m} \\ c &= 1.756 \times 10^{-8} \pm 5.323 \times 10^{-11}\,\mathrm{mGal/m^2} \end{aligned} \tag{39}$$

The uncertainties in these coefficients never cause an uncertainty in $\delta\Delta g^{\mathrm{NFSE}}$ larger than 0.5 μGal, for heights between 0 and 5000 m. If $\delta\Delta g^{\mathrm{NFSE}}$ is propagated through the Stokes integral, a height-dependent map of geoid errors due to this effect is obtained. Over the US, the impact of the near-field spherical effect has a root mean square (RMS) of 3 mm, but a maximum value of 7.5 cm in the Rocky mountains (Smith and Roman 2000). This is one clear example where Cartesian coordinates significantly fail to accurately approximate the terrain.

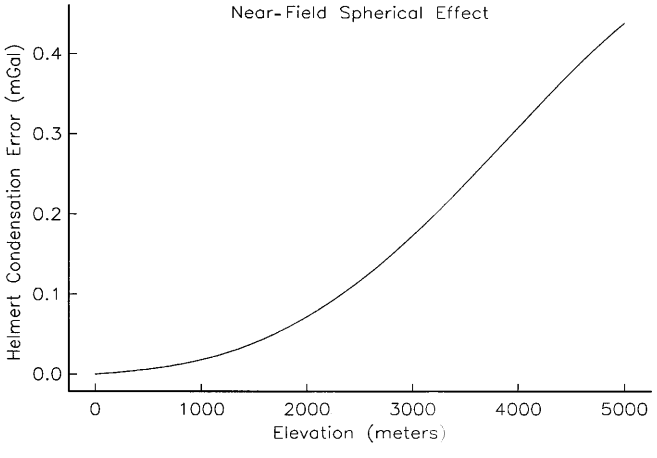

Fig. 7. Empirically derived errors in Helmert anomalies due to near-field spherical effects

As there is no closed form for the attraction of a condensed spherical prism, numerical integration was necessary for this test. For the central prism itself, special code was designed to break down the inner prism into rings of different radii, and perform a numerical integration over each ring. This allows the program to use coarse numerical integration far from the station's latitude and longitude, and fine numerical integration near the stations latitude and longitude.

5 Effect of using 3- vs 30-arcsecond data

In order to most effectively compute terrain effects in the space domain, it is best to know where more coarse (30-arcsecond) data may be substituted for finer resolution (3-arcsecond) data. To determine this, gravitational attraction was computed following the procedures in Sect. 4, but using 3-arcsecond data. The cumulative values for this case are presented in Figs. 8 and 9.

Notice that the agreement between the various models is much better for the 3-arcsecond data, as should be expected because the differences in the terrain models are smaller with the smaller-sized prisms. Also notice that all of the 3-arcsecond model results are within 1 mGal of the results of method 4 with the 30-arcsecond data. On all of the regions tested, the 30-arcsecond bilinear-top model was within 1 mGal of the 3-arcsecond result.

In the more rugged areas, the use of 3-arcsecond data provides a significant improvement in the model of the near-station topography. A large change is seen between the calculations for the flat-top prism models for the 3- and 30-arcsecond data for these areas, mostly concentrated in the prisms nearest to the station.

In order to determine where 30-arcsecond data may be used instead of 3-arcsecond data, the following plan was proposed. Assume, for an example, that the radius of $\psi = 3.5°$ represents an area outside of which we will compute the removal and restoration of the terrain in a separate way (Fast Fourier Transform methods or spherical harmonic representations, as examples) to that used inside the cap. This is the general approach being proposed at the NGS, and is the reason why this discussion has focused solely on computation of terrain effects inside a cap. For greatest computational speed, it would be best to use as coarse a DEM as possible inside much of the cap, while still retaining

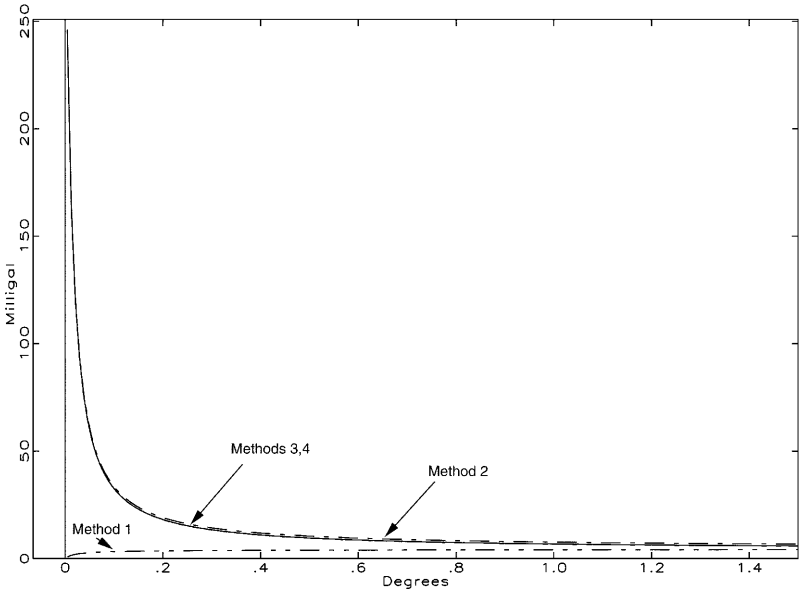

Fig. 8. As Fig. 5, but for 3-arcsecond terrain data. Same scale as Fig. 5

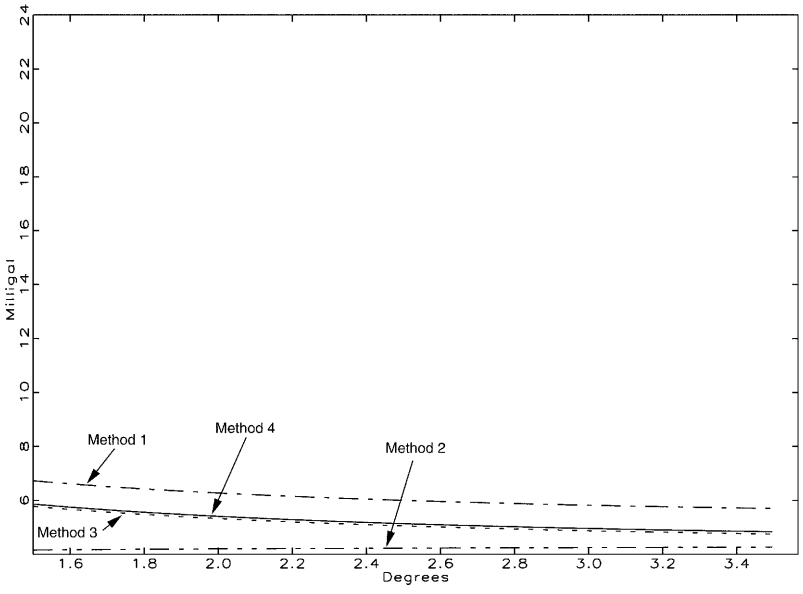

Fig. 9. As Fig. 6, but for 3-arcsecond terrain data. Same scale as Fig. 6

acceptable accuracy. Therefore in this example, if the cap radius is $\psi = 3.5°$, it is imperative to know how much of that cap can be 30-arcsecond DEM and how much must be 3-arcsecond DEM. Thus, it will be desirable to use a 3-arcsecond DEM from $\psi = 0°$ to $\psi = \psi'$ and a 30-arcsecond DEM from $\psi = \psi'$ to $\psi = 3.5°$, where ψ' is some cut-off radius to be determined. Figure 10 shows the relation between ψ' and the error difference between 30- and 3-arcsecond remove/restore computations.

It can be seen in Fig. 10 that if the error budget allows 10 μGal to be contributed from that part of the cap that has the 30-arcsecond DEM, then the ψ' value is 0.2°. In other words, we can use 3-arcsecond DEM inside $\psi = 0.2°$ and 30-arcsecond DEM from $\psi = 0.2$ to $\psi = 3.5°$ and suffer only a 10-μGal error from using the 30-arcsecond DEM. This hypothesis was tested for all four areas, and in each case $\psi = 0.2°$ was an acceptable radius for switching to 30-arcsecond data, presuming a 10-μGal error budget for using 30-arcsecond data inside a cap of 3.5°. The maximum cumulative error never exceeded 10-μGal. This is deemed acceptable, considering that the geoid impact of a 10-μGal systematic error made at every point throughout the Rocky mountains would only be 0.6 cm.

Similar methods could be used for determining at what point in using the 30-arcsecond data we can switch from bilinear tops to flat tops. It should be noted, however, that numerical integration is not significantly slowed by the addition of bilinear tops. As such, this question can remain unanswered, and bilinear tops kept as the norm throughout the process of computation. This will have no significant impact on speed, while allowing more rigorous accuracy to remain.

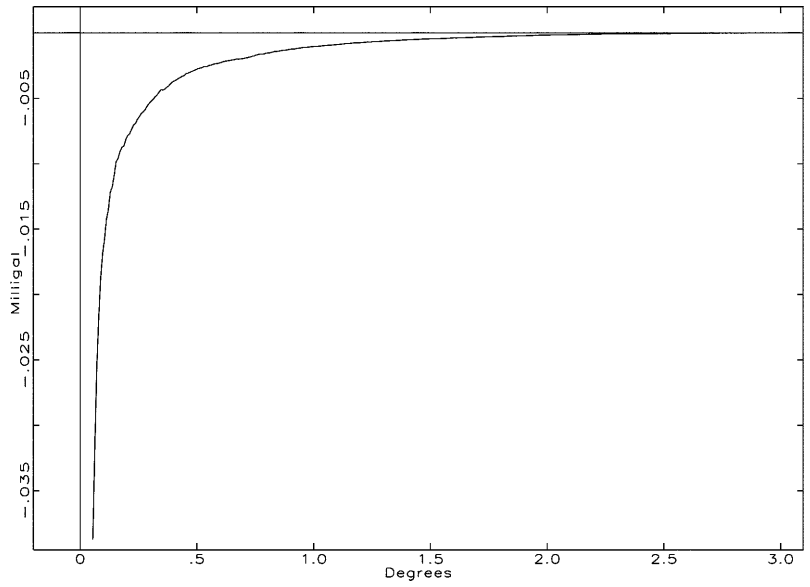

Fig. 10. Total error (mGal) of using 30-arcsecond DEM instead of a 3-arcsecond DEM between $\psi = \psi'$ and $\psi = 3.5°$, as a function of ψ', for central Colorado

It is quite unfortunate that an analytic solution to Eq. (12) [or (13)] has never been found (and may not even exist), as this generally means that numerical integration is the only highly accurate method for computing the gravitational attraction of localized prisms. As the distance between station and prism gets smaller, numerical integration (as a general rule) slows down significantly. Even if we were to switch to Cartesian coordinates near the station, the solution to the gravitational attraction of a bilinear-topped rectangular prism is not known in closed form, thus still requiring numerical integration. However, there is one possible way to gain quick (3-D) results, with a slight trade-off in accuracy (as high as 30 μGal, depending on station height): use triangular prisms, with sloped (planar, not curved) tops, in Cartesian coordinates (Smith 2000). Unfortunately, the issue of the near-field spherical effect can be only partly circumvented this way. Specifically, the greatest component of near-field spherical effect is due to the condensed, and not the 3-D mass differences. To completely remove the near-field spherical effect would require a fast solution to spherical condensed attraction.

6 Conclusions

It has been shown that the gravitational attraction of terrestrial masses and condensed masses, at a level consistent with recent geoid accuracy requirements, must be determined with greater rigor and with finer spatial resolution than has been used traditionally.

Use of spherical coordinates is necessary in order to remove two effects – one of incorrect volume (near-field) and the other of masses below the horizon (far-field). However, because no closed forms for the solution of gravitational attraction of spherical prisms have been solved, numerical integration is necessary. A Romberg algorithm has been found effective for this purpose.

Test computations at four gravity stations were performed. Variables investigated included coordinate system, shape of prism top, and DEM grid spacing. It was concluded that 3-arcsecond data with bilinear tops in spherical coordinates should be used for computing gravitational attractions inside a cap of 0.2°, and 30-arcsecond data with bilinear tops in spherical coordinates be used outside 0.2° to some critical radius. For a slight degradation in accuracy, the numerical integration over the spherical prisms closest to the gravity station may be replaced by closed forms, using Cartesian coordinates and sloped-top triangular prisms. The degradation of going from Cartesian to spherical coordinates is height dependent, ranging from 2 μGal for stations at 100 m elevation, all the way up to 431 μGal for stations at 5000 m elevation. These largest errors lead to as much as 7 cm of geoid error, and therefore it is concluded that no more than 50 μGal of error be considered acceptable. As such, it is suggested that near-field use of Cartesian coordinates be avoided for all terrain computations where elevations regularly exceed 1500 m.

Use of the traditional terrain correction is seen as undesirable as currently formulated, predominantly because of the dependence upon Cartesian coordinates, but also because the total remove-and-restore effects, for different locations of P and P_0, are combined into one computation. Because this one computation represents the removal of 3-D masses *at the surface*, and the restoration of condensed masses computed *at the geoid*, the assumption is that some downward continuation needs to be performed *between* these two effects. Without separating the remove-and-restore terms, the accuracy with which downward continuation may be computed is reduced.

Appendix

One question that has raised some debate amongst researchers has been the following: "In terms of Helmert's second method of condensation, what exactly does the terrain correction (TC) represent?" The answer (in

planar coordinates), to be proven below, is this: The TC is *exactly equal* to the combined effects of removing all of the 3-D topographic masses (computed at point P on the surface of the Earth) and the restoration of the 2-D condensed topographic masses (computed at point P_0 on the geoid). That is, in planar coordinates, the following will be proven:

$$\mathrm{TC} = -{}^{\mathrm{T}}g_P + {}^{\mathrm{C}}g_{P_0} \tag{A1}$$

where ${}^{\mathrm{T}}g_P$ is gravitational attraction at P (Earth's surface) due to topography and ${}^{\mathrm{C}}g_{P_0}$ is gravitational attraction at P_0 (geoid) due to condensed topography.

It will be shown by extension that the following is also true:

$$\mathrm{TC} \neq -{}^{\mathrm{T}}g_P + {}^{\mathrm{C}}g_P \tag{A2}$$

where ${}^{\mathrm{C}}g_P$ is gravitational attraction at P (Earth's surface) due to condensed topography.

The proof begins by writing some of the formulas that are needed. First, the attraction of all topographic masses in an infinite plane, above the geoid ($z = z_1$)

$${}^{\mathrm{T}}g_P = -G\rho \int_{x=-\infty}^{\infty} \int_{y=-\infty}^{\infty} \int_{z=z_1}^{z_2(x,y)} \frac{(z - z_P)}{l^3}\,\mathrm{d}z\,\mathrm{d}y\,\mathrm{d}x \tag{A3}$$

where

$$l = \sqrt{(x - x_P)^2 + (y - y_P)^2 + (z - z_P)^2} \tag{A4}$$

and removing the "z" integral analytically

$${}^{\mathrm{T}}g_P = -G\rho \int_{x=-\infty}^{\infty} \int_{y=-\infty}^{\infty} \left(\frac{1}{l_1} - \frac{1}{l_2}\right)\mathrm{d}y\,\mathrm{d}x \tag{A5}$$

where

$$\begin{aligned} l_1 &= \sqrt{(x - x_P)^2 + (y - y_P)^2 + (z_1 - z_P)^2} \\ l_2 &= \sqrt{(x - x_P)^2 + (y - y_P)^2 + (z_2(x,y) - z_P)^2} \end{aligned} \tag{A6}$$

Next we write out the formula for a Bouguer plate

$${}^{\mathrm{B}}A_P = -G\rho \int_{x=-\infty}^{\infty} \int_{y=-\infty}^{\infty} \int_{z=z_1}^{z_P} \frac{(z - z_P)}{l^3}\,\mathrm{d}z\,\mathrm{d}y\,\mathrm{d}x \tag{A7}$$

which becomes, after removing the z-integral

$${}^{\mathrm{B}}A_P = -G\rho \int_{x=-\infty}^{\infty} \int_{y=-\infty}^{\infty} \left(\frac{1}{l_1} - \frac{1}{l_0}\right)\mathrm{d}y\,\mathrm{d}x \tag{A8}$$

where

$$l_0 = \sqrt{(x - x_P)^2 + (y - y_P)^2} \tag{A9}$$

It should be noted that Eq. (A8) can be solved analytically to form the well-known formula for the attraction of a Bouguer plate

$${}^{\mathrm{B}}A_P = -2\pi G\rho(z_P - z_1) \tag{A10}$$

Now, finally, we write out the TC in its strictest definition. That is, the removal of masses above $z = z_P$ and the addition of masses below $z = z_P$ (Heiskanen and Moritz 1967, pp 131–132)

$$\mathrm{TC}_P = \begin{aligned} &-\left[-G\rho \int_{x=-\infty}^{\infty} \int_{y=-\infty}^{\infty} \int_{z=z_P}^{z_2} \frac{(z - z_P)}{l^3}\,\mathrm{d}z\,\mathrm{d}y\,\mathrm{d}x\right] \\ &\qquad \forall(x,y) \text{ s.t. } z_2(x,y) > z_P \\ &+\left[-G\rho \int_{x=-\infty}^{\infty} \int_{y=-\infty}^{\infty} \int_{z=z_2}^{z_P} \frac{(z - z_P)}{l^3}\,\mathrm{d}z\,\mathrm{d}y\,\mathrm{d}x\right] \\ &\qquad \forall(x,y) \text{ s.t. } z_2(x,y) < z_P \end{aligned} \tag{A11}$$

This formula holds as long as the topography is piecewise continuous. Further simplifying, we obtain

$$\mathrm{TC}_P = \begin{aligned} &-\left[-G\rho \int_{x=-\infty}^{\infty} \int_{y=-\infty}^{\infty} \int_{z=z_P}^{z_2} \frac{(z - z_P)}{l^3}\,\mathrm{d}z\,\mathrm{d}y\,\mathrm{d}x\right] \\ &\qquad \forall(x,y) \text{ s.t. } z_2(x,y) > z_P \\ &-\left[-G\rho \int_{x=-\infty}^{\infty} \int_{y=-\infty}^{\infty} \int_{z=z_P}^{z_2} \frac{(z - z_P)}{l^3}\,\mathrm{d}z\,\mathrm{d}y\,\mathrm{d}x\right] \\ &\qquad \forall(x,y) \text{ s.t. } z_2(x,y) < z_P \end{aligned} \tag{A12}$$

thus

$$\mathrm{TC}_P = -\left[-G\rho \int_{x=-\infty}^{\infty} \int_{y=-\infty}^{\infty} \int_{z=z_P}^{z_2} \frac{(z - z_P)}{l^3}\,\mathrm{d}z\,\mathrm{d}y\,\mathrm{d}x\right] \tag{A13}$$

and therefore

$$\mathrm{TC}_P = -G\rho \int_{x=-\infty}^{\infty} \int_{y=-\infty}^{\infty} \left(\frac{1}{l_2} - \frac{1}{l_0}\right)\mathrm{d}y\,\mathrm{d}x \tag{A14}$$

Examining Eqs. (A5), (A8), and (A14), we can see that the following is true:

$${}^{\mathrm{T}}g_P + \mathrm{TC}_P = {}^{\mathrm{B}}A_P \tag{A15}$$

or

$$\mathrm{TC}_P = -{}^{\mathrm{T}}g_P + {}^{\mathrm{B}}A_P \tag{A16}$$

This formula is nothing new. It is just a mathematical confirmation of the definition of the TC – that is, the difference between a Bouguer plate and the true topography. Turning our attention now to the gravitational attraction of condensed masses, the following formulas for P and P_0 are known [see Eqs. (27) and (30)]:

$$
\begin{aligned}
{}^{\mathrm{C}}g_P &= -G\rho \int_{x=-\infty}^{\infty} \int_{y=-\infty}^{\infty} \frac{(z_2 - z_1)(z_1 - z_P)}{l_1^3}\, \mathrm{d}y\, \mathrm{d}x \\
&= -G\rho(z_P - z_1) \int_{x=-\infty}^{\infty} \int_{y=-\infty}^{\infty} \frac{(z_2 - z_1)}{l_1^3}\, \mathrm{d}y\, \mathrm{d}x \qquad \text{(A17)}
\end{aligned}
$$

and

$$
\begin{aligned}
{}^{\mathrm{C}}g_{P_0} &= \lim_{z_P \to z_1} {}^{\mathrm{C}}g_P = -2\pi G\rho[z_2(x_P, y_P) - z_1] \\
&= -2\pi G\rho(z_P - z_1) = {}^{\mathrm{B}}A_P \qquad \text{(A18)}
\end{aligned}
$$

[this formula is in agreement with the limiting form of Eqs. (1–17a) in Heiskanen and Moritz (1967)]. Unless $z_2 = z_P$ everywhere (i.e. the topography was in fact, before condensation, an infinite flat Bouguer plate), then the following must also hold:

$$
{}^{\mathrm{C}}g_P \neq {}^{\mathrm{B}}A_P \qquad \text{(A19)}
$$

As such, we can substitute Eqs. (A18) and (A19) into (A16) to yield the following equality and inequality:

$$
\mathrm{TC}_P = -{}^{\mathrm{T}}g_P + {}^{\mathrm{C}}g_{P_0} \qquad \text{(A20)}
$$

and

$$
\mathrm{TC}_P \neq -{}^{\mathrm{T}}g_P + {}^{\mathrm{C}}g_P \qquad \text{(A21)}
$$

Note that this proof is for planar coordinates only, and does not rely on the approximation formula of the TC [Eq. (37)], but rather on strict definitions of the various terrain components in planar coordinates.

References

Blais JAR, Ferland R (1983) Optimization in gravimetric terrain corrections. Can J Earth Sci 21(5): 505–515

Heiskanen WA, Moritz H (1967) Physical geodesy. Freeman WH, San Francisco

Helmert FR (1884) Mathematical and physical theories of higher geodesy. Teubner, Leipzig

Lambert WD (1930) The reduction of observed values of gravity to sea level. Bull Geod 26: 107–181

Leaman DE (1998) The gravity terrain correction. Expl Geophys 29: 467–471

Ma XQ, Watts DR (1994) Terrain correction program for regional gravity surveys. Comput Geosci 20(6): 961–972

Martinec Z (1998) Boundary-value problems for gravimetric determination of a precise geoid. Lecture notes in Earth sciences, vol 73. Springer, Berlin Heidelberg New York

Martinec Z, Matyska C, Grafarend EW, Vaníček P (1993) On Helmert's 2nd condensation method. J Geod 18: 417–421

Martinec Z, Vaníček P, Mainville A, Veronneau M (1996) Evaluation of topographical effects in precise geoid computation from densely sampled heights. J Geod 70: 746–754

Milbert DG, Smith DA (1998) Implications of spherical Earth models for gravity reduction procedures and geoid computation. Poster presentation at the Autumn meeting of the American Geophysical Union, San Francisco. Available online at: http://www.ngs.noaa.gov/GEOID

Moritz H (1968) On the use of the terrain correction in solving Molodensky's problem. Rep 108, Department of Geodetic Science, The Ohio State University, Columbus

Nagy D (1966) The gravitational attraction of a right rectangular vertical prism. Geophysics 21(2): 362–371

Press WH, Teukolsky SA, Vetterling WT, Flannery BP (1992) Numerical recipes in Fortran, 2nd edn. Cambridge University Press, Cambridge

Sideris MG (1984) Regional geoid determination. In: Vaníček, Christou (eds) Geoid and its geophysical interpretations. CRC Press, Boca Raton, pp 77–94

Sjöberg LE, Nahavandchi H (1999) On the indirect effect in the Stokes–Helmert method of geoid determination. J Geod 73: 87–93

Smith DA (1992) The use of high resolution height data in the computation of high precision geoid undulations on the island of Maui. Rep 424, Department of Geodetic Science and Surveying, The Ohio State University, Columbus

Smith DA (2000) The gravitational attraction of any polygonally shaped vertical prism with inclined top and bottom faces. J Geod 74(5): 414–420

Smith DA, Milbert DG (1999) The GEOID96 high resolution geoid height model for the United States. J Geod 73(5): 219–236

Smith DA, Roman DR (2000) Recent advances in the acquisition and use of terrain data for geoid modeling over the United States. In: Schwarz RP (ed) J Geodesy Beyond 2000, International Association of Geodesy Symposia vol. 121, Springer Verlag, pp 107–111, 2000. Proc IUGG99, Birmingham, UK, 19–30 July 1999

Smith DA, Roman DR (in press) A new high resolution digital elevation model for the Northwest United States. Surv Land Inf Syst

Vaníček P, Kleusberg A (1987) The Canadian geoid – Stokesian approach. Manuscr Geod 12: 86–98

Véronneau M (1997) The GSD95 geoid model for Canada. In: Segawa J, Fujimoto H, Okubo S (eds). Proc Gravity, Geoid and Marine Geodesy, Tokyo, 30 September–5 October 1996. IAG symposia vol 117. Springer, pp 573–580

Wolfram S (1999) The mathematica book. Wolfram Media, Champaign, IL